Quantitative Analysis of Cadmium Selenide Nanocrystal Concentration by Comparative Techniques

ARTICLE *in* ANALYTICAL CHEMISTRY · JANUARY 2008

Impact Factor: 5.64 · DOI: 10.1021/ac0715064 · Source: PubMed

5 AUTHORS, INCLUDING:

Sara Cavaliere
Université de Montpellier
46 PUBLICATIONS **1,544** CITATIONS
SEE PROFILE

Thomas Nann
Victoria University of Wellington
126 PUBLICATIONS **4,682** CITATIONS
SEE PROFILE

Anal. Chem. **2007,** *79,* 8987−8993

Quantitative Analysis of Cadmium Selenide Nanocrystal Concentration by Comparative Techniques

Erol Kuçur,[†] Frank M. Boldt,[†] Sara Cavaliere-Jaricot,[†] Jan Ziegler,[‡] and Thomas Nann*[,‡]

Freiburg Materials Research Centre (FMF), Albert-Ludwigs University, Stefan-Meier-Strasse 21, D-79104 Freiburg, Germany, and School of Chemical Sciences and Pharmacy, University of East Anglia (UEA), Norwich NR4 7TJ, U.K.

In this paper, we compared atomic absorption spectroscopy (AAS), anodic stripping voltammetry (ASV), and UV−vis spectroscopy for the determination of the concentration of CdSe nanocrystal (NC) solutions. The experimental results were combined with crystallographic calculations of the NC size, which led to a very accurate determination of the nanocrystal concentration—a crucial parameter for bioanalytical applications. Furthermore, such a combined approach can be extended to the determination of shell thickness of core/shell materials (e.g., CdSe/ZnS).

In the past decade, semiconductor nanocrystals (NCs)—so-called quantum dots or QDs—became attractive tools for biolabeling[1,2] and electro-optical applications, due to their superior optical properties.[3−8] For complex biological experiments, such as quantifying target molecules by specific nanobio interactions, highly luminescent and stable fluorescent labels are required.[13] Since an excess of both nanocrystals and biomolecules must be avoided for coupling reactions, it is very important to know the concentration of the nanocrystals beforehand. The concentration of NCs is extremely difficult measure, nevertheless, because their extinction coefficients are difficult to determine and they vary for each particle size.[9−12] Besides the remarkable success of NCs in the biological application field, they opened also new possibilities to improve photovoltaic devices and light-emitting diodes.[14−23] It was predicted that charge transfer to NCs from conducting polymers can be greatly enhanced by direct grafting of the polymers onto nanocrystals. Recently made progress in the synthesis of oligomeric ligands and grafting them onto the surface of semiconductor nanocrystals improved the electrical connection to the nanocrystals without having an exact knowledge of the nanocrystal concentration.[3−8] Since the determination of the nanocrystals' concentration by MALDI-TOF (matrix-assisted laser desorption/ionization time-of-flight) is still very difficult,[24−26] and the exact knowledge, particularly the concentration of the different compounds in nanocrystal/polymer composites, should be necessary for an improved charge-transfer knowledge, a new, easy to use, and accurate way is introduced in this paper.

This publication deals with the determination of the overall nanocrystal concentration in one-batch-based synthesis. By comparing different concentration measurement techniques, namely, atomic absorption spectroscopy (AAS), anodic stripping voltammetry (ASV), and UV−vis, the best solution is concluded by

* To whom correspondence should be addressed. E-mail: T.Nann@uea.ac.uk. Fax: +44(0)1603 593985.

[†] Albert-Ludwigs University.

[‡] University of East Anglia.

(1) Gao, X.; Cui, Y.; Levenson, R. M.; Chung, L. W. K.; Nie, S. *Nat. Biotechnol.* **2004**, *22*, 969−976.
(2) Seleverstov, O.; Zabirnyk, O.; Zscharnack, M.; Bulavina, L.; Nowicki, M.; Heinrich, J.-M.; Yezhelyev, M.; Emmrich, F.; O'Regan, R.; Bader, A. *Nano Lett.* **2006**, *6*, 2826−2832.
(3) Aldakov, A.; Chandezon, F.; De Bettignies, R.; Firon, M.; Reiss, P.; Pron, A. *Eur. Phys. J. Appl. Phys.* **2007**, *36*, 261−265.
(4) Zhang, H.; Wang, C.; Li, M.; Ji, X.; Zhang, J.; Yang, B. *Chem. Mater.* **2005**, *17*, 4783−4788.
(5) Skaff, H.; Sill, K.; Emrick, T. *J. Am. Chem. Soc.* **2004**, *126*, 11322−11325.
(6) Zhang, H.; Cui, Z.; Wang, Y.; Zhang, K.; Ji, X.; Lü, C.; Yang, B.; Gao, M. *Adv. Mater.* **2003**, *15*, 777−780.
(7) Skaff, H.; Ilker, M. F.; Coughlin, E. B.; Emrick, T. *J. Am. Chem. Soc.* **2002**, *124*, 5729−5733.
(8) Kucur, E.; Riegler, J.; Urban, G. A.; Nann, T. J. *Chem. Phys.* **2004**, *120*, 1500−1505.
(9) Yu, W. W.; Qu, L.; Guo, W.; Peng, X. *Chem. Mater.* **2003**, *15*, 2854−2860.
(10) Schmelz, O.; Mews, A.; Basché, T.; Herrmann, A.; Müllen, K. *Langmuir* **2001**, *17*, 2861−2865.
(11) Striolo, A.; Ward, J.; Prausnitz, J. M.; Parak, W. J.; Zanchet, D.; Gerion, D.; Milliron, D.; Alivisatos, A. P. *J. Phys. Chem. B* **2002**, *106*, 5500−5505.
(12) Leatherdale, C. A.; Woo, W.-K.; Mikulec, F. V.; Bawendi, M. G. *J. Phys. Chem. B* **2002**, *106*, 7619−7622.
(13) Ghazani, A. A.; Lee, J. A.; Klostranec, J.; Xiang, Q.; Dacosta, R. S.; Wilson, B. C.; Tsao, M. S.; Chan, W. C. W. *Nano Lett.* **2006**, *6*, 2881−2886.
(14) Tang, A.-W.; Teng, F.; Gao, Y.-H.; Li, D.; Zhao, S.-L.; Liang, C.-J.; Wang, Y.-S. *J. Lumin.* **2007**, *122−123*, 649−651.
(15) Xuan, Y.; Pan, D.; Zhao, N.; Ji, X.; Ma, D. *Nanotechnology* **2006**, *17*, 4966−4969.
(16) Steckel, J. S.; Snee, J.; Coe-Sullivan, S.; Zimmer, J. P.; Halpert, J. E.; Anikeeva, P.; Kim, L.-A.; Bulovic, V.; Bawendi, M. G. *Angew. Chem.* **2006**, *35*, 5828−5931.
(17) Caruge, J.-M.; Halpert, J. E.; Bulovic, V.; Bawendi, M. G. *Nano Lett.* **2006**, *6*, 2991−2994.
(18) Achermann, M.; Petruska, M. A.; Koleske, D. D.; Crawford, M. H.; Klimov, V. *Nano Lett.* **2006**, *6*, 1396−1400.
(19) Kumar, S.; Nann, T. *J. Mater. Res.* **2004**, *19*, 1990−1994.
(20) Robel, I.; Subramanian, V.; Kuno, M.; Kamat, P. V. *J. Am. Chem. Soc.* **2006**, *128*, 2385−2393.
(21) Liu, D.; Kamat, P. V. *J. Phys. Chem.* **1993**, *97*, 10769−10773.
(22) Arici, E.; Hoppe, H. Schäffler, F.; Meissner, D.; Malik, M. A.; Sariciftci, N. S. *Thin Solid Films* **2004**, *451−452*, 612−618.
(23) Wang, P.; Abrusci, A.; Wong, H. M. P.; Svensson, M.; Andersson, M. R.; Greenham, N. C. *Nano Lett.* **2006**, *6*, 1789−1793.
(24) Gaumet, J.-J.; Strouse, G. F. *J. Am. Soc. Mass. Spectrom.* **2000**, *11*, 338−344.
(25) Khitrov, G. A.; Strouse, G. F. *J. Am. Chem. Soc.* **2003**, *125*, 10465−10469.
(26) Kuzuya, T.; Tai, Y.; Yamamuro, S.; Sumiyama, K. *Chem. Phys. Lett.* **2005**, *407*, 460−463.

10.1021/ac0715064 CCC: $37.00
Published on Web 10/31/2007

discussing the advantages and disadvantages of each. Furthermore, a new crystallographic model is introduced with the aim to enhance the accuracy of the approximation of the total amount of atoms in one NC.

EXPERIMENTAL SECTION

Chemicals. The following chemicals were used for the synthesis of CdSe nanocrystals: cadmium oxide (CdO, 99.998% Alfa Aesar), stearic acid (≥98.5%, Fluka), trioctylphosphine oxide (TOPO, 99%, Aldrich), trioctylphosphine (TOP, 95% Fluka), hexadecylamine (HDA, ≥99% Fluka), selenium powder (Se, 99.5% Aldrich), and succinic acid (99.5% Fluka). The nanocrystal synthesis was performed by a low-temperature method, which is described in detail together with the shelling procedure of CdSe nanocrystals with ZnS in the Supporting Information. After the end of the reaction, 10 mL of dry methanol was added to start the flocculation of the obtained nanocrystals. The yielded NCs were centrifuged and redispersed in 8 mL of chloroform. This washing process was repeated until the cadmium precursors were completely removed from the final solution, as previously proved by Yu et al.[9]

Chemicals for AAS or ASV measurements were HNO_3 (>69.5%, Fluka), cadmium ICP/AA standard solution (Aldrich), mercury(II) nitrate (97%, Merck), and sodium acetate (99%, Grüssing). All buffers and stock solutions were prepared from Milli-Q water (Millipore Corp.). Commercially available NCs were purchased from Evident Technologies. Since the used solvent has an influence on the spectroscopic characteristics, the NCs were transferred to hexane, a solvent with zero dipole moment. This influence is determined by spectral shifts of the absorption and/or luminescence spectrum and is mainly caused by the dipole characteristics of the solvent.[27,28]

Measurement Setup. The UV−vis and photoluminescence spectra were recorded on a J&M TIDAS diode array spectrometer, which was calibrated by taking into account the diode sensibility and the excitation intensity. The wavelength was calibrated with a standard fluorescence set obtained from the Federal Institute for Materials Research and Testing, Berlin (www.bam.de). Additional absorbance spectra were taken with a quartz tungsten halogen (7.5 W)/deuterium (35 W) combined light source. A J&M FL3095 monochromator with a 75 W ozone-free xenon bulb was used for the monochromatic light source.

Anodic stripping voltammetric measurements were performed in a homemade three-electrode electrochemical inert gas cell controlled by a PG 340 potentiostat−galvanostat (HEKA, Germany). An in situ plated mercury-coated glassy-carbon electrode (1 mm diameter) was used as the working electrode, a platinum wire as the counter electrode, and a Ag/AgCl electrode as the reference electrode. The measurement solution (2 mL volume) consisted of a 0.2 M acetate buffer (pH 5.5) containing 0.1 mM mercury(II) nitrate.

Concentration Measurements by Atomic Absorption Spectroscopy. For the determination of the final Cd concentration, 50 μL of the washed CdSe nanocrystal solution was placed in a test tube. This solution was heated up to 150 °C with a heat gun until the solvent evaporated completely. Subsequently, 40 μL of HNO_3 (>69.5%) was added to the dried pellet to dissolve the nanocrystals completely. This procedure was assisted with an ultrasonic bath. The volume of this solution was filled up to 2 mL with Milli-Q water. The AAS measurement was performed on a Perkin-Elmer 4110 Zeeman atomic absorption spectrometer.

The accuracy of the AAS measurement was obtained by repeated measurements of two different stock solutions containing 0.4 and 1.2 mg/mL cadmium. A standard deviation of 0.03 mg/mL was calculated.

Concentration Measurements by Anodic Stripping Voltammetry. The preliminary preparation of the CdSe nanocrystal solution for the determination of the Cd concentration by ASV was the same as described above for the AAS measurements. After that, 20 μL of the diluted solution of dissolved nanocrystals was transferred into 2 mL of the measurement solution. To perform differential pulse voltammetric measurements, the pretreatment of the glassy-carbon electrode was 60 s at 0.6 V, with an accumulation time of 240 s at −1.4 V and a rest period time of 30 s without stirring. The determination of the Cd concentration using the standard addition mode with three stock solutions (200 ppb Cd ions) occurred with a step potential of 50 mV, a pulse amplitude of 20 mV, and a sampling time of 40 ms. The measurements showed a standard deviation of 0.15 mg/mL.

Concentration Measurements by UV−Vis Spectroscopy. UV−vis methods from the literature shall be discussed briefly, for a better comparison with other methods. The concentration determination introduced by Yu et al. was obtained through the measurement of a CdSe stock solution.[9] This solution was diluted until the first absorbance maximum ($1S(e)-1S_{3/2}(h)$ transition) was below an optical density of 0.3. Subsequently, the concentration of the nanocrystal solution was calculated by taking into account the empirically determined extinction coefficient of CdSe nanocrystals together with the path length of the light (1 cm Hellma cuvette, QS 101) and the wavelength at the first absorbance peak. A further correction factor as stated in the publication was also taken into account.[9] Starting from the concentration of the dilute solution in the cuvette, calculations were performed to obtain the concentration of the stock solution.

Yu et al. and Schmelz et al. determined the nanocrystal concentration by dissolving them with HNO_3 and taking into account ideal spheres with the CdSe bulk density.[9,10] The sizes of the nanocrystals were determined by transmission electron microscopy (TEM) and by absorption measurements. The concentration was measured by means of AAS. Striolo et al. performed the concentration measurements by drying the centrifuged thoroughly washed nanocrystal pellet and weighing and dispersing them in a certain amount of toluene.[11]

Introduction of the Crystallographic Model. Depending on the conversion factor of the synthesis, concentration calculations were performed based on the nanocrystal size calculation established by Dushkin et al., which is a modification of the Brus formula (see the Supporting Information). Those formulas describe the energy of an exciton in the first ground state depending on the size of the semiconductor nanocrystal. The modified formula has a higher accuracy than the original formula by Brus et al. and other groups (see the Supporting Information and ref

(27) Wang, Y.; Herron, N. *J. Phys. Chem.* **1991**, *95*, 525−532.
(28) Yu, K.; Zaman, B.; Singh, S.; Wang, D.; Ripmeester, J. A. *Chem. Mater.* **2005**, *17*, 2552−2561.

Table 1. Summary of the Synthesis Parameters, the First Absorption Peak Wavelength, the Emission Wavelength, and the fwhm for the Same Duration Synthesis at Different Temperatures (A−C) and for Different Duration Synthesis Times at One Temperature (D−E)[a]

experiment no.	temp/°C at 120 min	first absorption /nm	wavelength /nm	fwhm /nm
A	160	520	557	27
B	180	541	583	32
C	200	580	622	40
	synthesis time/ min at 180 °C			
D	20	540	562	29
E	40	542	573	29
F	80	545	580	30

[a] The values for A−F are mean values with a total number of five experiments for each synthesis. The standard deviation for those is 2−3%.

29).[29−34] Dushkin et al. performed their calculations by modifying the initial formula given by Brus et al. with an additional penetrating depth of the exciton into the organic passivation layer. We calculated the nanocrystal size from the emission spectrum and estimated the amount of NCs by taking the conversion factor of the synthesis into account. The Cd concentration was determined by either AAS or ASV and the amount of Cd atoms in each nanocrystal, which was calculated using the software Diamond 3.0. Initial calculations with a spherical nanocrystal model and bulk material values, like effective mass and density, revealed insufficient concentration values based upon a mass deviation for the same wavelength. Thus, we used the crystallographic model stated in the Supporting Information (detailed information about the introduction and validation of this model can be found in the Supporting Information).

RESULTS

CdSe nanocrystal experiments with same synthesis time but different growth temperature (experiments A−C, see Table 1) and same temperature but different growth time (experiments D−F, see Table 1) were performed for the investigation of the concentration dependence on the conversion factor. Such results are depicted in Table 1. The emitting wavelength varied between 557 and 622 nm for the syntheses performed at different temperatures and between 562 and 580 nm for the syntheses at constant temperature. The full width at half-maximum (fwhm) varied between 27 and 40 nm.

ASV measurements with cadmium stock solutions and measurements of the experiments A−C are depicted in Figure 1. Sensibility tests for ASV measurements revealed a linear behavior in the range of 100−1000 ppb. The measured current at −0.75 V increases by a higher synthesis temperature, from which a higher cadmium value can be deduced.

The results of the differently measured concentrations for these nanocrystal solutions are summarized in Table 2. The average values and standard deviations were calculated by taking five measurements for each technique into account. As one can see, the ASV measurements are in good agreement with the AAS measurements. Both clearly show Cd concentrations below the maximum limit of 1.4 mg/mL for experiments A−C and 1.75 mg/mL for experiments D−F, whereas the data from the ASV measurements revealed a larger standard deviation. The concentration determination by the UV−vis method based on the calculations of Yu et al. showed a much higher Cd concentration in the solution compared to the ASV and AAS data.[9] Those concentrations even exceeded the maximum initial amount of Cd in the solution.

Due to the different synthesis parameters, especially because of the low-temperature one-pot synthesis, we expected different conversion values for the experiments performed. For example, the higher the synthesis temperature is, the higher the conversion value should be (see Table 3). This behavior should also be observed for a longer synthesis time. In Table 3 the behavior of the former can be observed for both AAS and ASV measurements. By comparing the data obtained from the AAS measurements with the ASV ones, the former are lower for both synthesis parameters. However, at a higher temperature (experiment C, see Table 3) the result is the inverse. This fact can be attributed to the casual errors undertaken by the operator.

DISCUSSION

Before comparing the results obtained with different temperature synthesis techniques, the conversion factor for low temperatures should be considered carefully. As depicted in Figure 2 the conversion factor increases with both time and temperature. By increasing the temperature, the conversion of the initial Cd amount to nanocrystals is accelerated, which can be seen by the increasing measurement current in Figure 1B. Assuming a high-temperature-based synthesis, one can expect that the conversion factor reaches nearly 100% after several minutes. This fact is also valid for a hot-injection-based synthesis. Thus, the synthesis temperature plays an important role for the synthesis reaction rate of the nanocrystals, their quality, and their concentration. Regarding the latter comparison of the various presented synthesis techniques, one has to additionally remark that not only the conversion factor but also the quality of the nanoparticles strongly depends on the purity grades of the chemicals, which therefore should be as high as possible.[9,36]

After the determination of the conversion factor by means of AAS, the nanoparticle concentrations were determined by factoring the number of Cd atoms per nanocrystal of relevant size (A−F) into the calculation. These values were calculated with the crystallographic program "Diamond" (see the Supporting Information). The exponential fitting curve for the total amount of cadmium atoms (y) in one nanocrystal at a given emission wavelength (nm) is stated below (eq 1):

$$y_{Cd} = 0.0952 \exp(0.0168\lambda), \quad R^2 = 0.9914 \qquad (1)$$

(29) Dushkin, C.; Papazova, K.; Dushkina, N.; Adachi, E. *Colloid Polym. Sci.* **2005**, *284*, 80−85.
(30) Brus, L. *J. Phys. Chem.* **1986**, *90*, 2555−2560.
(31) Wang, Y.; Herron, N. *J. Phys. Chem.* **1991**, *95*, 525−532.
(32) Kayanuma, Y. *Solid State Commun.* **1986**, *59*, 405−408.
(33) Nosaka, Y. *J. Phys. Chem.* **1991**, *95*, 5054−5058.
(34) Kayanuma, Y. *Phys. Rev. B* **1988**, *38*, 9797−9804.
(35) Lippens, P. E.; Lannoo, M. *Phys. Rev. B* **1989**, *39*, 10935−10942.
(36) Nann, T.; Riegler, J. *Chem. Eur. J.* **2002**, *8*, 4791−4794.

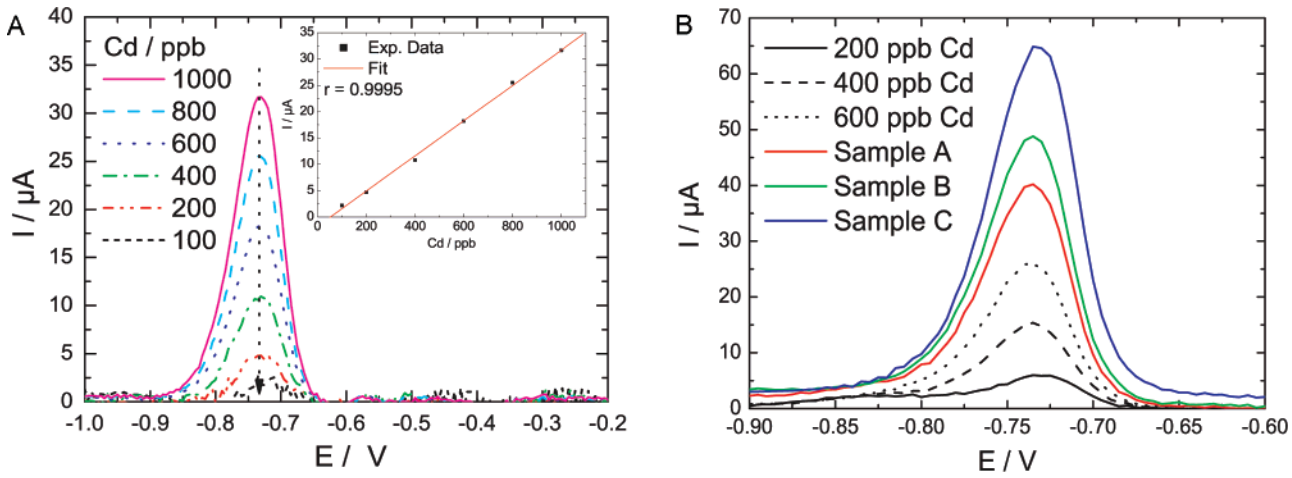

Figure 1. (A) Anodic stripping voltammetry (ASV) calibration measurement done by subsequent addition of cadmium stock solution. The inset graph shows the detection linearity in the range of 100−1000 ppb. (B) ASV measurement data of experiments A−C.

Table 2. Experimental Results of the CdSe Concentration from the Six Different Synthesis Setups Obtained by ASV, AAS, and Calculations Acquired by UV−Vis Measurements by Using the Empirically Obtained Extinction Coefficient[a]

	ASV/mg/mL		AAS/mg/mL		UV−vis/mg/mL	
experiment no.	mean	SD	mean	SD	mean	SD
A	0.88	0.06	0.83	0.02	14.58	0.09
B	1.15	0.08	1.04	0.03	6.90	2.06
C	1.22	0.19	1.39	0.04	6.20	1.20
D	0.93	0.09	0.91	0.03	10.72	1.29
E	1.17	0.23	1.08	0.03	17.88	1.29
F	1.51	0.23	1.31	0.04	12.37	0.09

[a] Through the initial weight (40 mg CdO = 35 mg Cd) a maximum value of 1.4 mg/mL (vol 25 mL) and 1.75 mg/mL (vol 20 mL) is theoretically possible for synthesis A−C and D−F, respectively.

Table 3. Conversion Factor of the Different Synthesis Parameters A−C and D−F Determined by ASV and AAS, Respectively

	conversion factor/%	
experiment no.	ASV	AAS
A	46	41
B	73	62
C	80	97
D	15	13
E	39	30
F	73	53

A summary of the concentration calculations can be found in Table 4. By increasing the temperature (A−C) the concentration of nanocrystals decreases, whereas the increase of the synthesis time (D−F) produces a higher nanocrystal concentration. The former result can be explained by the initial amount of nuclei that varies with temperature. Furthermore, the increased synthesis rate and thus the accelerated Ostwald ripening process, which can be deduced from the widened fwhm (Table 1), plays an important role. When the fwhm of QDs obtained for different reaction times (D−F) are compared with those obtained at different temperatures

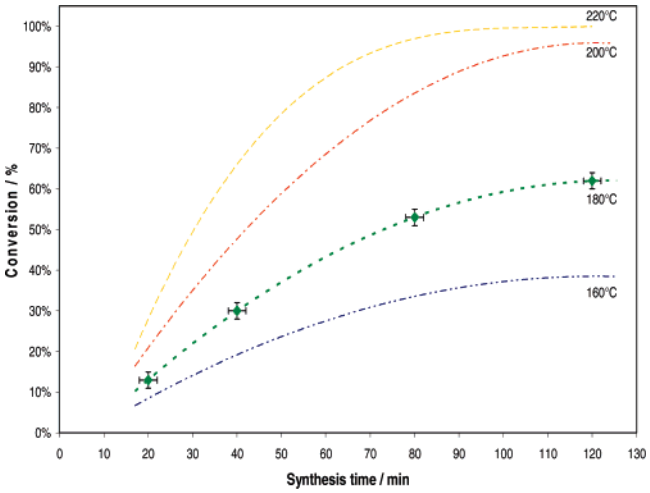

Figure 2. Conversion factor vs synthesis time at a constant temperature of 180 °C measured with AAS (green diamonds). The error bars in the *x*-scale represent the uncertainty of the operator, whereas the error bars in the *y*-scale represent the error of the AAS measurements. The dotted lines are guidelines for the eyes. Furthermore, predictions upon data from initial experiments of the behavior of the conversion factor depending on the temperature are also depicted (220 °C, orange dash line; 200 °C, red dash-dot line; 160 °C, blue dash-dot-dot line).

(A−C), one can conclude that Ostwald ripening has not occurred yet. Therefore, the turning point for the amount of nanocrystals has not been reached at 180 °C for 80 min yet. This assumption is consistent with the nanocrystals concentration calculated and depicted in Table 4. Besides this, one can point out that the use of high-purity chemicals and this gentle synthesis route results in a nearly 100% conversion.

The exact knowledge of the concentration facilitates the design of the conjugates or polymer/NC composites and thus minimizes the risks of undefined parameters in the system. For a fundamental work toward this, Table 5 compares the nanocrystal concentrations obtained with a combined technique of AAS and theoretical calculations and UV−vis techniques from the literature.[9−12] The concentration determination was performed by taking the extinction coefficient into account. As one can see, the concentration determined by the UV−vis technique presented here is different from the results obtained by the listed separately

Table 4. Summary of the Concentration Calculations for Differently Sized Nanocrystals A−F[a]

	no. of Cd atoms per NC	conversion factor/%	converted no. of Cd atoms	no. of NC	concn (no. NC/L)	concn (μmol NC/L)
A	592	41	6.83×10^{19}	1.15×10^{17}	4.61×10^{18}	0.191
B	842	62	1.03×10^{20}	1.23×10^{17}	4.91×10^{18}	0.204
C	1622	97	1.62×10^{20}	9.96×10^{16}	3.98×10^{18}	0.165
D	830	13	2.16×10^{19}	2.61×10^{16}	1.30×10^{18}	0.043
E	858	30	5.00×10^{19}	5.82×10^{16}	2.91×10^{18}	0.097
F	902	53	8.83×10^{19}	9.79×10^{16}	4.89×10^{18}	0.162

[a] The amount of Cd atoms per nanocrystal was obtained by the software Diamond. The conversion factor was taken from the previously obtained AAS data.

Table 5. Comparison between the Different Concentration Methods Obtained by a Combination of AAS Measurements and Theoretical Calculations and Concentrations Calculation Obtained by the Use of Empirical Found Extinction Coefficient[a]

	concentration (μmol NC/L)			
	AAS plus theor calculations	UV−vis ref 9	UV−vis ref 10	UV−vis ref 11
A	0.191	4.76	1.95	0.20
B	0.204	2.26	0.81	0.10
C	0.165	2.04	0.74	0.22
D	0.043	1.90	0.84	0.10
E	0.097	2.77	0.60	0.08
F	0.162	2.01	0.86	0.12

[a] Refs 9−11.

Table 6. Summary of the Results Obtained with Several Concentration Determination Techniques for Commercially Available CdSe Obtained from Evident Technologies[a]

	concentration (μmol NC/L)				
	Evident	AAS plus theor calculations	UV−vis ref 9	UV−vis ref 10	UV−vis ref 11
Evidot 500	n.a.	2.68×10^{-3}	11.4	5.29	0.39
Evidot 520	n.a.	2.35×10^{-3}	9.54	3.15	0.31
Evidot 545	1.41×10^{-7}	1.32×10^{-3}	5.98	2.31	0.27
Evidot 570	1.23×10^{-7}	9.70×10^{-4}	4.11	2.39	0.28
Evidot 595	9.32×10^{-8}	1.12×10^{-3}	2.61	1.69	0.50
Evidot 620	3.71×10^{-8}	7.21×10^{-4}	1.29	1.32	0.33

[a] The concentrations for Evident nanoparticles were calculated by taking into account the total number of Cd and Se atoms for each size concentration values given by Evident Technologies (1.3, 1.4, 1.61, 2.1 mg/mL for Evidot 545, 570, 595, 620 nm, respectively).

introduced techniques. This variation arises from the differently determined varying extinction coefficients. The extinction coefficient determined from Leatherdale et al. was calculated at an absorbance wavelength of 350 nm and thus will not be considered any further.[12] The nanocrystal concentration determined by Yu et al. and Schmelz et al. gives a higher concentration than the method presented here.[9,10] Only the extinction coefficient and thus the concentration determined by Striolo et al. seems to be comparable to the presented results.[11] The origin of this big discrepancy lies first in the difficulty of the determination of the extinction coefficient and second in the separating procedure of the nanocrystals from the precursors still present in the synthesis solution. If the latter is not thoroughly performed, the calculation of the concentration will give values with a high error. Yu et al.'s uncertainty value of 20−30% prerequisites a thorough washing procedure before determination of the extinction coefficient.[9] Due to the large discrepancies from different work groups, it is also conceivable that the extinction coefficient of nanocrystals in comparison to organic fluorophores is additionally a function of the crystal quality. High crystallinity, i.e., fewer defects, guarantees higher quantum yields. Since the quantum yield of nanocrystals is strongly influenced by surfactants, their coverage rate to nanocrystals will differ not only the photoluminescence characteristic but also conceivably the absorption cross section. This can lead to a different extinction coefficient. Hence, nanocrystals prepared by different syntheses should be compared carefully, even if they have similar shaped absorption characteristics.

Besides this comparison one should concentrate on the analysis of the different syntheses (A−F). The nanocrystal concentration decreases by increasing the temperature (A−C) and increases by a longer synthesis time (D−F). The former result is explained by different achieved wavelength, thus the different nanocrystal sizes and the initial stock solution of Cd. Since the Ostwald ripening process did not occur in the synthesis series (D−F), some initial precursors are still left for further growing on the existing nanocrystals and more preferably for building new nanocrystals. After the complete reaction of the initial precursors, Ostwald ripening will take place presumably and hence reduce the nanocrystal concentration. Unfortunately, this concentration behavior in the experiments D− F could not be revealed by any UV−vis method (see Table 5).

Outlook: Applicability to Other CdSe Nanocrystals. Commercially available differently sized CdSe nanocrystals were purchased from Evident Technologies and diluted to the same absorption coefficient as was done previously. The absorption spectra revealed clear band transitions. The results from the measurement of the nanocrystal concentrations are summarized in Table 6. First, one can notice that the large discrepancy between the UV−vis and AAS results is still present. The extinction coefficient determined from Striolo et al. results in the most accurate concentration compared to the other UV−vis methods and the concentration values measured here. The concentration values given by Evident Technologies were calculated for the used solutions by taking into account the amount of Cd and Se atoms of each NC batch. The size was calculated by the modified formula from Dushkin et al. (see the Supporting Information) using the "crystal" model based upon UV−vis measurements. It is clear that the concentration obtained by the method presented here revealed

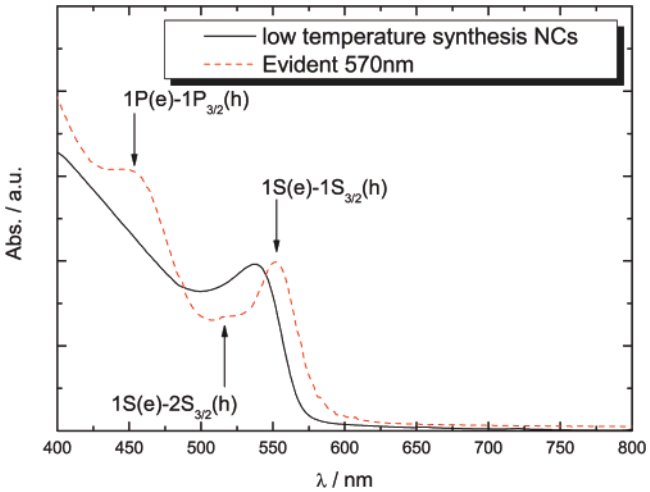

Figure 3. Absorption spectra of Evident 570 nm nanocrystals (red dotted line) and low-temperature-synthesized nanocrystals (black solid line).

a smaller value compared to the several UV−vis methods but a higher value compared to the values calculated from Evident Technologies specifications. Since the AAS measurement revealed a high accuracy in the former experiments (see Tables 2 and 5) one has to investigate more about the origin of this noticeable variation.

By comparing the absorption spectra from the CdSe synthesis presented herein and the Evident CdSe nanocrystals, one's attention is attracted by the fact that Evident CdSe do have more intense, prominent absorption transitions, e.g., $1S(e)-1S_{3/2}(h)$ (first absorption peak), $1S(e)-2S_{3/2}(h)$, and $1P(e)-1P_{3/2}(h)$, than the NCs made by the low-temperature synthesis (see Figure 3).

This characteristic might arise from the crystallinity grade as well as from the different ligands on the surface of the nanocrystals and thus from the effective absorption cross section of the nanocrystals. Unless the ligands of the Evident nanoparticles remain unclear, the consideration of a different absorption cross section due to different ligands might lead to a false conclusion. For the sake of completeness, it has to be mentioned that the nanocrystal-dissolving protocol was optimized for the synthesis used here. An essential prerequisite for the AAS measurement is a complete dissolving of the nanocrystal. Thus, together with the uncertainty about the Evident NC ligands, the probably incomplete dissolution of the Evident nanocrystals with our protocol might lead to not comparable results.

By considering the different photoluminescence and absorption spectra, Evident nanocrystals revealed a much higher absorption value at a certain concentration for the highest photoluminescence value compared to the nanocrystals synthesized here. Besides this fact, they do have a low photoluminescence signal. Especially the small nanoparticles showed also a deep trap emission characteristic at lower energy regions at room temperature, which was not detectable with the nanocrystals produced here. Due to those characteristics, one concludes that low-temperature-synthesized CdSe nanocrystals reveal a different absorption characteristic and accordingly a different extinction coefficient. By use of the latter in the past, the use of the concentration determination by UV−vis for the presented nanoparticle synthesis routes will lead to a discrepancy between the measured concentration and the real concentration.[9−12] On the basis of these investigations, we deduce that the extinction coefficient might depend on the synthesis procedure, on the used capping ligands, and thus on the crystallinity or quality of the nanocrystals (work in progress).

Table 7. Summary of the Spectroscopic Data Obtained from Measurements of CdSe/ZnS Core/Shell NCs and ZnSe NC in Hexane Together with the Differently Determined Diameters of Each[a]

solvent: hexane	CdSe/ZnS	ZnSe
first absorption peak/nm	573	n.a.
emission/nm	589	429
fwhm/nm	36	48
calcd diameter/nm	4.44	5.38
measd diameter/nm	4.3	n.a.
amount of Cd atoms per NC	1443	n.a.
amount of Zn atoms per NC	1015	2051

[a] Additionally, the amount of cadmium and zinc atoms per NC is also depicted.

Applicability to CdSe/ZnS Core/Shell Nanocrystals. Because of the instability characteristics of bare CdSe nanocrystals, e.g., the high sensitivity toward oxygen, those nanocrystals are mainly shelled with ZnS, a material with a higher band gap and less sensitivity.[37] The higher band gap material provides a stronger confinement of the excitons inside the core material, whereby a higher stability of the photoluminescence characteristics is achieved. The shell thickness can be determined by TEM measurements, through the measurement of the core material diameter before and after the shelling process.[38] Due to the fact that the core material continues to grow during the surface modification, and conucleation of presumably CdS, ZnS, or ZnSe is taking place, a comparison of the different TEM diameters before and after shelling process is related with a high uncertainty.[38] A better possibility is given by subtracting the calculated diameter of the core from the TEM diameter of the core/shell nanoparticle, whereas the prior was done by taking into account the absorption peak and the size calculation formula.[29] The spectroscopic investigation of the core/shell material revealed a second emission peak at 429 nm besides the main emission peak at 589 nm (Supporting Information). The latter is assigned to CdSe/ZnS, whereas the prior is assigned to ZnSe, which grew during the shell process by reaction of unused Se precursor with the injected Zn precursor. ZnS can be excluded due to their main emission characteristics in the deep blue region (up to 330 nm). Those parameters are depicted together with the calculated and measured diameters in Table 7.

Another way to determine the correct shell thickness can be done by combining the determined cadmium amount of the sample via ASV or AAS together with the actual amount of cadmium atoms inside a nanocrystal. The ASV measurement of CdSe/ZnS core/shell material dissolved in HNO_3 is depicted in Figure 4. One can see that the peak current of cadmium (−0.75 V) rises without affecting the zinc peak (−1.17 V) after the addition of cadmium stock solution.

(37) Katari, J. B.; Colvin, J. B.; Alivisatos, A. *J. Phys. Chem.* **1994**, *98*, 4109−4117.
(38) Ziegler, J.; Merkulov, A.; Grabolle, M.; Resch-Genger, U.; Nann, T. *Langmuir* **2007**, *23*, 7751−7759.

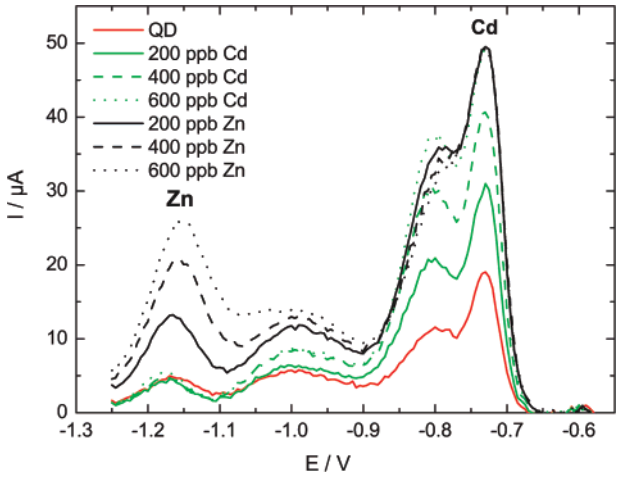

Figure 4. Anodic stripping voltammetry (ASV) measurements of CdSe/ZnS core/shell nanocrystals (red line, "QD") and subsequently added stock solutions (200 ppb) of Cd and Zn, respectively.

Table 8. Comparison of the Results Obtained from ASV and AAS Measurements for CdSe/ZnS Core/Shell Nanocrystals

	ASV	AAS
amount of Cd atoms	7.80×10^{18}	6.38×10^{18}
amount of Zn atoms	5.70×10^{18}	2.00×10^{19}
amount of CdSe NC	5.41×10^{15}	5.69×10^{15}
amount of Zn atoms in ZnSe	2.15×10^{17}	7.55×10^{17}
amount of Zn atoms in CdSe/ZnSe	5.48×10^{18}	1.92×10^{19}
amount of Zn per CdSe NC	1015	3383
monolayer (ML) of ZnS	1.34	3.12

The determination of the amount of Zn in the ZnSe or CdSe/ZnS nanoparticles, respectively, was done by an initial coarse approximation putting the area of both emission characteristics in relation (see the Supporting Information). This ratio (~0.38) was multiplied with the total detected amount of Zn atoms (see Table 7) to get the amount of Zn in the ZnSe nanoparticles (see Table 8). For a more accurate calculation of the concentration, and thus the right ratio, the extinction coefficients of both materials have to be taken into account. Since this determination is still afflicted with uncertainties, the coarse approximation shall be satisfying enough.

The ZnS shell thickness was calculated with 1.34 ML for the AAS data by separating the free Zn amount from the existing CdSe nanocrystals concentration, which was calculated by using the model introduced above. The calculation was supported by building up one ZnS monolayer after another with the use of the crystal model. Measurements by TEM combined with core diameter determination by spectroscopic data revealed a shell thickness of 0.8 ML ($r_{ZnS} = 0.3$ nm). This comparison shows that the determination of the ZnS shell thickness is even possible with the initial coarse approximation made here. Hence, additional work has to be done to solidify the proof of the applicability and to enhance the introduced technique.

CONCLUSION

The determination of the nanocrystal concentration was improved by taking a new theoretical model for calculation of the nanocrystal size in combination with AAS measurements into account. Furthermore, ASV measurements confirmed the AAS data very well. Comparison of the results with extinction coefficients and thus concentrations obtained by UV−vis spectroscopy as commonly performed in the literature revealed large discrepancies. We attribute this to the different nanocrystals' absorption cross sections from different synthesis routes. Furthermore, the initial coarse determination of the shell thickness of CdSe/ZnS core/shell material based upon the calculations and crystal model was confirmed by a comparison with TEM measurements.

ACKNOWLEDGMENT

The authors thank William Yu, Xiaogang Peng, Moungi G. Bawendi, and Frank S. Riehle for helpful discussions. E.K., S.C.-J., and J.Z. thank the German Ministry for Education and Research (BMBF) for financial support within the Projekts 13N8846 (FLUOPLEX) and 13N8792 (SUN-LED). The first two authors contributed equally to this work.

SUPPORTING INFORMATION AVAILABLE

More information about the synthesis, the nanoparticle properties (TEM, XRD), the introduction to the crystallographic model and its validation. This material is available free of charge via the Internet at http://pubs.acs.org.

Received for review July 17, 2007. Accepted September 21, 2007.

AC0715064